Proceedings of the 10th International Conference on Civil Structural and Transportation Engineering (ICCSTE 2025)
July, 2025 | Imperial College London Conference Center, London, United Kingdom
Paper No. 141
DOI: 10.11159/iccste25.141

Strength of Corroded RC Circular Columns Repaired with Advanced Composites

Feras AbuObaida[1], Farid Abed[2], Ahmed El Refai[3], Tamer El Maaddawy[1]
[1]United Arab Emirates University
Al Ain, UAE
201770001@uaeu.ac.ae; tamer.maaddawy@uaeu.ac.ae
[2] American University of Sharjah
Sharjah, UAE
fabed@aus.edu
[3] Laval University
Quebec City, Canada
ahmed.elrefai@gci.ulaval.ca

Abstract **–** The feasibility and viability of two different composite-based repaired solutions, namely carbon fabric-reinforced cementitious matrix (C-FRCM) and carbon fiber-reinforced polymer (C-FRP) composites to repair axially-loaded reinforced concrete (RC) circular column pre-damaged by reinforcement corrosion are examined in this paper. Four RC circular columns were tested. One RC column was neither corroded nor repaired to act as a benchmark. Three RC columns were subjected to accelerated corrosion which rendered 13% and 37% cross-sectional losses in the longitudinal steel reinforcement and the steel ties, respectively. One corroded RC column was tested to failure without repair. Two corroded RC columns were repaired with 2 layers of C-FRCM and C-FRP composites in the hoop direction, then tested to failure. The corroded-unrepaired column exhibited a 34% reduction in the load carrying capacity. Both composite-based repair solutions were able to recover the original strength of the control column without increasing the column's stiffness. Although the strength of the C-FRP confined column was 53% higher than that of its counterpart repaired with C-FRCM composites, its ductility index was 26% lower.

Keywords**:** columns; circular; corrosion; repair; FRP; FRCM.

1. Introduction

Reinforced concrete (RC) columns in severe environments are susceptible to deterioration and performance degradation due to corrosion of the steel reinforcement. Corrosion damage in RC columns compromises the integrity of the concrete cover and reduces the area of the longitudinal and transverse steel reinforcement, thus decreasing the load carrying capacity of the columns [1-3]. Traditionally, RC jacketing has been employed to repair corroded RC columns [4]. In addition to being labor-intensive, conventional RC jacketing lacks aesthetic appeal. It increases the column's cross-section and reduces the available space [4]. Furthermore, the RC jacketing technique is often vulnerable to corrosion damage when exposed to aggressive environments, which would require repeated cycles of repairs [4]. Advanced materials in the form of fiber-reinforced polymer (FRP) and fabric-reinforced cementitious matrix (FRCM) composites utilize nonmetallic reinforcement embedded into a polymeric/cementitious matrix with a reduced thickness, thus offering promising alternative solutions for rehabilitation of RC columns [5, 6].

Previous studies verified the effectiveness of epoxy-based FRP wraps as a corrosion protection system capable of reducing the corrosion rate in RC columns exposed to harsh environmental conditions [7-14]. Nevertheless, little is known about the feasibility and viability of using FRP wraps to improve the load carrying capacity of RC columns pre-damaged by corrosion. In most of previous studies, FRP wraps have been installed prior to exposure to accelerated corrosion or at a minor corrosion level less than 10% [7-10]. Practical applications would involve rehabilitation of RC columns pre-damaged by corrosion of various severity. Very few studies examined the behavior of RC columns pre-damaged by corrosion then repaired with FRP wraps [11-15]. Although these studies provided promising results and interesting findings, the specimens were very small-sized [11], without steel ties in the test region [12], and/or repaired without the removal and replacement of

the deteriorated concrete cover prior to the application of FRP wraps [11-15]. Such a repair methodology does not resemble what might be encountered in filed conditions.

The FRCM repair solution employes a cementitious matrix as a binder, which alleviates concerns related to the toxicity and reduced fire resistance of the epoxy matrix used in FRP composites [5]. Carbon (C)-FRCM wraps can be used in RC columns for impressed current cathodic protection and structural strengthening (ICCP-SS) simultaneously [16, 17]. The dual-function ICCP-SS system employing C-FRCM composites has a potential to decrease the corrosion rate and increase the load carrying capacity of RC columns [16, 17]. More studies are needed to verify the effectiveness of the ICCP-SS solution, because in one of these studies [16], the degree of reinforcement corrosion was not measured, while in the other study [17], the degree of reinforcement corrosion was in the range of 1.2% to 4% only. For RC columns with such a small level of corrosion, it would be difficult to draw meaningful conclusions. Pre-cracked RC columns wrapped with FRCM composites exhibited superior performance relative to that of a benchmark column that was neither cracked nor strengthened [18-20]. Typically, failure of FRCM composites initiates by interfacial debonding at the fabric-matrix interface and/or slippage of the fabrics within the matrix, which hinders full utilization of the tensile strength of the fabrics and limits the gain in the load carrying capacity [5, 18-20]. The inclusion of fan-type FRP anchors in the FRCM repair solution could delay deboning/slippage of the fabrics and further improve the strength by up to 21% relative to that of similar FRCM-confined columns without anchors [21]. The strength of plain concrete cylinders wrapped with FRCM composites was less than that of similar cylinders wrapped with FRP [22]. To date, no information is available on the behavior of RC columns pre-damaged by corrosion then repaired with FRCM composites.

The limited information on rehabilitation of RC columns with corroded reinforcement using advanced composite materials warrants further research. This paper presents sample results of an ongoing comprehensive research work developed by the authors, which aimed at quantifying the effect of corrosion on the response of RC circular columns and examining the behavior of RC circular columns pre-damaged by corrosion then repaired with two different composite-based solutions, namely FRCM and FRP.

2. Experimental Program

Results of four axially loaded RC circular columns are reported in this paper. The test matrix is provided in Table 1. One column, D0-NR, was neither corroded nor repaired to act as a benchmark. The other three columns were subjected to accelerated corrosion for 60 days under an impressed current of 1000 mA, which corresponded to 13% and 37% cross-section losses in the longitudinal steel reinforcement and the steel ties, respectively. At the end of the accelerated corrosion process, column D1-NR was tested to failure without repair, whereases columns D1-FRM and D1-FRP were repaired with 2 layers of C-FRCM and C-FRP wraps, respectively, then tested to failure under uniaxial compression.

Table 1: Test matrix

Specimen designation	Corrosion Damage (%) [a]		Number of C-FRP/C-FRCM layers
	Longitudinal steel	Steel ties	
D0-NR	0	0	0
D1-NR	13	37	0
D1-FRM	13	37	2
D1-FRP	13	37	2

[a] Cross-sectional loss based on measured diameters of corroded steel coupons after rust removal according to ASTM G1-03 [23].

2.1. Test Specimens

Fig. 1 shows details of a typical test specimen. The columns were designed according to ACI 318-19 [24] to behave as short columns. The specimens consisted of a column segment with end stubs to provide anchorage for the column's longitudinal bars and mitigate the risk of premature failure at the column's ends. The column segment had a circular cross section with a diameter of 200 mm and a clear height of 800 mm. Each end stub had a height of 200 mm and a square cross section of 400×400 mm. The column was reinforced with 6 No. 12 (12 mm diameter) longitudinal bars providing a longitudinal steel reinforcement ratio of 2.2%. The steel ties were No. 8 (8 mm diameter) with a center-to-

center spacing of 150 mm and a clear cover of 20 mm. The end stubs were heavily reinforced to maximize their rigidity and ensure the occurrence of failure in the column segment. A longitudinal stainless-steel tube was placed in the center throughout the length of the column segment and passed through the top end stub to act as a cathode during the accelerated corrosion process. The stainless-steel tube and the longitudinal steel bars were extended out of the specimen to facilitate making of the electrical connections during the accelerated corrosion. The extended parts of the reinforcement were cut off prior to structural testing.

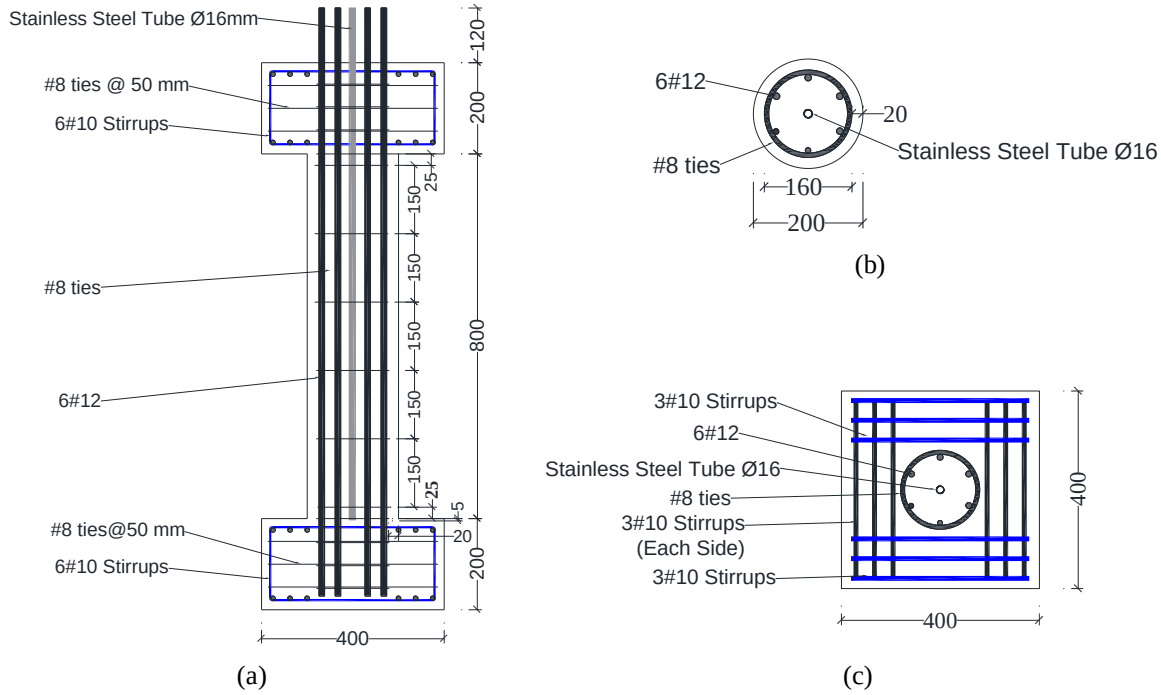

Fig. 1. A schematic showing details of a typical test specimen: (a) longitudinal section; (b) column's cross-section; (c) end-stub's cross-section (dimensions are in mm).

2.2. Materials

A normal-strength concrete with a measured cylinder strength of f_c' = 26 MPa was used to construct test specimens. The concrete mixture used to cast the column segment included 5% NaCl (salt) by the weight of cement to depassivate the steel bars and promote corrosion. The 12 mm diameter steel reinforcing bars had a yield strength (f_y) of 560 MPa and an ultimate strength (f_u) of 672 MPa. The 8 mm diameter steel ties had f_y of 580 MPa and f_u of 640 MPa. A non-shrink cementitious grout with f_c' = 35 MPa was used to replace the deteriorated concrete cover of the corroded-repaired columns. The carbon fiber sheets used in the C-FRP repair solution were unidirectional (Fig 2a) with a tensile modulus of 230 GPa, a tensile strength of 3900 MPa, an ultimate elongation of 1.5%, and a nominal thickness of 0.17 mm [25]. The carbon fiber sheets were impregnated and bonded to the concrete surface using an epoxy adhesive provided by the manufacturer. The carbon fabrics used in the C-FRCM repair solution consisted of unidirectional carbon fiber strands (Fig. 2b) with a center-to-center spacing of 17 mm, a tensile modulus of 240 GPa, a tensile strength of 4300 MPa, an ultimate elongation of 1.75%, and an equivalent thickness of 0.157 mm [26]. A commercial cementitious mortar provided by the manufacturer was used to produce the C-FRCM composites. A typical cured C-FRCM composite layer has a tensile strength of 970 MPa, an ultimate tensile strain of 0.0125, and a cracked tensile modulus of elasticity of 75 GPa [27].

2.3. Repair Methodology

The repair process is summarized in Fig. 3. It involved the removal of the deteriorated concrete cover, roughening of the concrete substrate and surface cleaning of the corroded steel bars using a waterjet, placement of a non-shrink cementitious grout to retain the original shape of the column's cross section, and application of C-FRCM/C-FRP composite wraps in the circumferential direction of the column's cross section. The surface of the column segment was roughed again using a waterjet prior to the application of C-FRCM composites. The surface of the columns repaired with C-FRP composites was cleaned of dust and smoothened prior to the application of the C-FRP wraps. A wet layup process was adopted to install the composite layers around the cross section of the column's segment. The columns repaired with C-FRCM composites were covered with plastic sheets for 24 hours, moist-cured for 28 days using burlaps, then left air-cured until the time of the structural testing was reached. The columns repaired with C-FRP composites were left air-cured until the time of structural testing was reached.

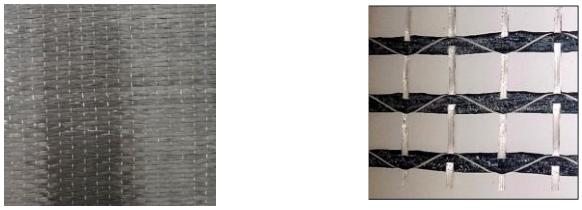

(a) (b)

Fig. 2. Carbon fibers used: (a) carbon fiber sheets used in C-FRP repair; (b) carbon fiber strands used in C-FRCM repair.

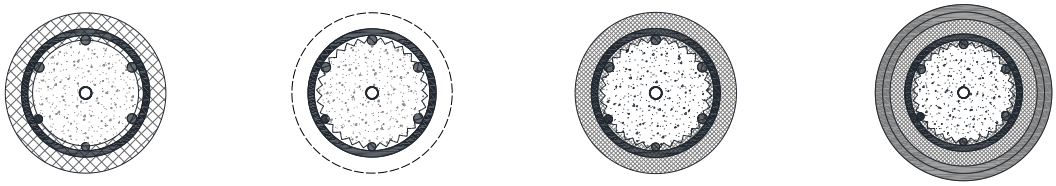

(a) (b) (c) (d)

Fig. 3. Repair process of corroded columns: (a) identification of damaged areas; (b) removal of deteriorated concrete cover and surface preparation; (c) placement of non-shrink cementitious grout; (d) application of C-FRCM/C-FRP wraps.

2.4. Test Setup and Instrumentation

All columns were tested under displacement-controlled loading at a rate of 0.3 mm/min using a Universal Testing Machine (UTM). The loads and axial displacements were obtained from the UTM readings. Strain gauges (SGs) were bonded to the steel reinforcement in the longitudinal and hoop directions. Additional SGs were bonded to the outermost surface of the column at mid-height to measure the longitudinal compressive strain. Furthermore, SGs were also bonded to carbon fibers in the hoop direction. A digital data acquisition system was used to record the readings.

3. Experimental Results

Corrosion of the steel reinforcement resulted in longitudinal cracks with a maximum width of 0.4 mm parallel to the longitudinal steel bars and transverse cracks with a maximum width of 0.1 mm parallel to the steel ties. Test results in terms of failure modes, load-displacement response, load carrying capacity, and strain measurements are discussed in this section.

3.1. Failure Mode

The control column D0-NR exhibited longitudinal cracks that were initiated at the column's mid-height then propagated toward both ends. Next, spalling of the concrete cover occurred in discrete locations along the column's

length (Fig. 4a). The corroded unrepaired column D1-NR was already pre-cracked because of corrosion of the steel reinforcement. As the applied axial compression force increased during testing, the vertical cracks continued to develop and widen. Next, the concrete cover spalled gradually leaving a large area of the steel reinforcement exposed (Fig. 4b). Column D1-FRM displayed no concrete cover spalling; however, multiple longitudinal cracks were initiated in the outermost layer of the cementitious mortar (Fig. 4c). These longitudinal cracks widened significantly as the load progressed. Detachment of the external mortar layer due to interfacial debonding at the fabric-mortar interface was observed, particularly at the top portion of the column segment (Fig. 4c). Column D1-FRP failed suddenly due to tensile rupturing of the C-FRP in the hoop direction at the mid-height of the column (Fig. 4d). The rupture of the C-FRP was accompanied by a loud noise.

(a) (b) (c) (d)

Fig. 4. Failure mode: (a) D0-NR; (b) D1-NR; (c) D1-FRM; (d) D1-FRP.

3.2. Load-Axial Displacement Relationship

Fig. 5 shows the load versus the axial displacement relationships of the tested columns. All columns exhibited a quasilinear response in the pre-peak stage. Column D1-NR exhibited a reduced axial stiffness because of the presence of corrosion cracks. The stiffness of the repaired columns did not exceed that of the control column. Column D1-NR reached its peak load at an axial displacement value lower than that of the control column D0-NR. The behavior of column D1-FRM in the pre-peak stage coincided with that of the control column D0-NR. The axial displacement of D0-NR and D1-FRM at the peak load was identical. In contrast, column D1-FRP exhibited more than three-fold increase in its axial displacement at peak load relative to that of D0-NR. It is noteworthy that column D1-FRP exhibited a displacement hardening when the load reached a value almost equals to the ultimate load of control column D0-NR, thus implying activation of the confinement produced by the C-FRP wraps. The tested columns exhibited different behaviors in the post-peak stage. Columns D0-NR and D1-FRP exhibited a sudden drop in load at peak. In contrast, columns D1-NR and D1-FRM exhibited a softening branch in the post-peak stage with a gradual stiffness degradation. The ductile behavior exhibited by column D1-NR could be ascribed to the gradual spalling of the pre-cracked concrete cover, whereas that of column D1-FRM could be attributed to the gradual interfacial debonding that occurred at the fabric-mortar interface prior to final failure.

3.3. Load Capacity and Ductility

A summary of the experimental test results is presented in Table 2. The load capacity of D1-NR with reinforcement corrosion was 66% of that of the control column D0-NR. The strength of column D1-FRM was the same as that of the control column D0-NR, whereas that of D1-FRP exceeded that of the control column by 52%. The strength gain, with respect to the load capacity of column D1-NR, caused by the C-FRP repair solution (131%) was higher than that caused by the C-FRCM repair solution (51%). In this study, the ductility index (DI) was calculated as the ratio of the strain at a post-peak load value of 85% of the ultimate load to the yield strain, which was defined by the intersection of two characteristic lines; the first line was the secant slope passing through load-displacement curve at 75% of the ultimate load and the second line was constant at the ultimate load value [28]. Despite the reduction in its load carrying capacity, the DI of column D1-NR was 1.5 times

that of the control column D0-NR. Although column D1-FRM reached its peak load at an axial displacement value equal to that of D0-NR, it exhibited an improved DI with a value 71% higher than that of D0-NR. Furthermore, the DI of D1-FRM was approximately 1.4 that of D1-FRP.

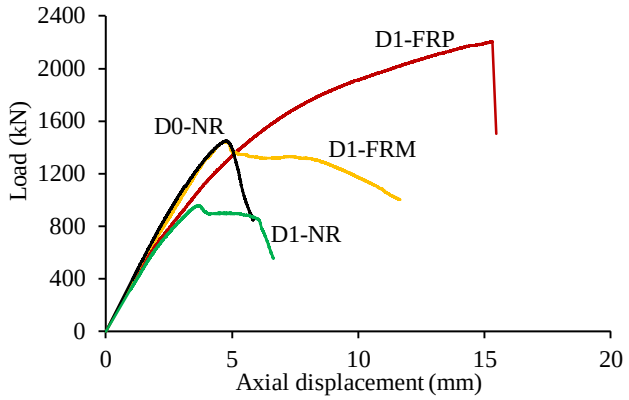

Fig. 5. Load vs axial displacement.

Table 2: Test results

Specimen	Ultimate load (kN)	Strength ratio [a,b]	Displacement at peak (mm)	Ductility index (DI)
D0-NR	1448.11	-	4.75	1.28
D1-NR	956.60	0.66	3.65	1.95
D1-FRM	1445.38	1.00 (51%)	4.74	2.19
D1-FRP	2206.10	1.52 (131%)	15.31	1.61

[a.] The strength ratio is calculated with respect to the strength of D0-NR.
[b.] Values between parentheses represent the gain in strength with respect to that of D1-NR.

3.4. Strain Measurements

Results of the SG measurements at peak load are summarized in Table 3. The longitudinal and hoop steel strain readings for column D0-NR were not recorded due to damage to the SGs prior to testing. At peak load, the longitudinal steel bars in columns D1-NR and D1-FRM reached 78% and 90% of the steel yield strain, respectively. The corresponding strains in the steel ties were approximately 7% and 32% of the yield strain. In contrast, the steel strains of both the longitudinal reinforcement and the ties exhibited by column D1-FRP at peak load exceeded the yield strain. The improved confinement provided by the C-FRP wraps allowed the longitudinal steel reinforcement and the ties to develop their full tensile strength prior to failure. The control column D0-NR reached its peak load at a longitudinal concrete compressive strain value of 3162 με, which coincided with the design value of the ultimate concrete strain specified by the ACI 318-19 [24]. Column D1-NR exhibited a reduced longitudinal concrete compressive strain at peak lead, probably because of the presence of longitudinal corrosion cracks prior to testing. The longitudinal surface compressive strain of column D1-FRM at peak load was almost the same as that of D0-NR, whereas the hoop strain in the fibers was 2525 με, which corresponded to 21% of the limiting value (12,000 με) specified by the ACI 549.6R-20 [5]. Such small strain values reported for column D1-FRM could imply a premature/early interfacial debonding at the fabric-mortar interface. These findings are consistent with other published data which documented the inferior performance of the C-FRCM jacketing relative to that of the C-FRP wraps, due to the poor adhesion and absence of a strong chemical bond between the carbon fibers and the cement-based matrices [22]. In contrast, column D1-FRP exhibited significant surface strains in the longitudinal and hoop directions at peak load, which further verified the effectiveness of the confinement provided by the C-FRP wraps. The longitudinal surface compressive strain exhibited by column D1-FRP prior to failure was close to the limiting value (10,000 με) specified by the ACI 440.2 [6] for FRP-

confined concrete. The hoop fiber strain exhibited by column D1-FRP at peak load was approximately $0.51\varepsilon_{fu}$, where ε_{fu} = ultimate tensile strain of CFRP. The hoop fiber strain exhibited by column D1-FRP prior to failure is in agreement with the limiting value of the effective fiber strain ($0.55\varepsilon_{fu}$) specified by the ACI 440.2 [6] for FRP-confined concrete.

Table 3: Strains at peak load

Specimen	Longitudinal compressive strain (με)		Hoop tensile strain (με)	
	Longitudinal steel strain	Outermost surface strain	Strain in steel ties	Strain in carbon fibers
D0-NR	NA	3162	NA	-
D1-NR	2190	2271	195	-
D1-FRM	2512	3265	890	2525
D1-FRP	4472	8813 [a]	2970	7683

[a.] Measured at 84% of the ultimate load.

4. Conclusion

- The reduction in the load carrying capacity of RC circular columns was more significant than the level of corrosion damage in the longitudinal steel reinforcing bars. The column with 13% corrosion in the longitudinal steel bars exhibited a strength reduction of 34% relative to that of the control column.
- It was feasible to repair RC circular columns with C-FRCM and C-FRP jacketing solutions considering removal and replacement of the deteriorated concrete cover prior to the application of the composite-based materials.
- The C-FRCM repair solution was able to recover the original strength of the control column. The load capacity of the column repaired with C-FRP jacketing exceeded that of the control column by 52%.
- Although the load capacity of the column repaired with C-FRCM jacketing was 66% of that of its counterpart repaired with C-FRP jacketing, its ductility index was 36% higher.

Acknowledgments

The authors would like to acknowledge the financial support provided by the UAE University (Fund No. 12N172).

References

[1] Z. Cui and A. Alipour, "Concrete cover cracking and service life prediction of reinforced concrete structures in corrosive environments," *Construction and Building Materials*, vol. 159, pp. 652–671, Jan. 2018, doi: 10.1016/j.conbuildmat.2017.03.224.

[2] J. Xia, W. Jin, and L.-Y. Li, "Performance of Corroded Reinforced Concrete Columns under the Action of Eccentric Loads," *Journal of Materials in Civil Engineering*, vol. 28, p. 04015087, Jun. 2015, doi: 10.1061/(ASCE)MT.1943-5533.0001352.

[3] Hameed, A., Afzal, M. F. U. D., Javed, A., Rasool, A. M., Qureshi, M. U., Mehrabi, A. B., & Ashraf, I., "Behavior and Performance of Reinforced Concrete Columns Subjected to Accelerated Corrosion," *Metals*, vol. 13, no. 5, Art. no. 5, May 2023, doi: 10.3390/met13050930.

[4] S. Raza, M. K. I. Khan, S. J. Menegon, H.-H. Tsang, and J. L. Wilson, "Strengthening and Repair of Reinforced Concrete Columns by Jacketing: State-of-the-Art Review," *Sustainability*, vol. 11, no. 11, Art. no. 11, Jan. 2019, doi: 10.3390/su11113208.

[5] ACI Committee 549, ACI 549.6R-20: Guide to Design and Construction of Externally Bonded Fabric-Reinforced Cementitious Matrix (FRCM) and Steel-Reinforced Grout (SRG) Systems for Repair and Strengthening Masonry Structures, *Technical Documents*, Nov. 2020.

[6] ACI Committee 440, ACI PRC-440.2-23: Design and Construction of Externally Bonded Fiber-Reinforced Polymer (FRP) Systems for Strengthening Concrete Structures—Guide, *Technical Documents*, Nov. 2023.

[7] T. El Maaddawy, A. Chahrour, and K. Soudki, "Effect of Fiber-Reinforced Polymer Wraps on Corrosion Activity and Concrete Cracking in Chloride-Contaminated Concrete Cylinders," *Journal of Composites for Construction*, vol. 10, no. 2, pp. 139–147, Apr. 2006, doi: 10.1061/(ASCE)1090-0268(2006)10:2(139).

[8] A. S. Debaiky, M. F. Green, and B. B. Hope, “Carbon Fiber-Reinforced Polymer Wraps for Corrosion Control and Rehabilitation of Reinforced Concrete Columns,” *ACI Materials Journal*, 2002.
[9] Lee, C., Bonacci, J. F., Thomas, M. D., Maalej, M., Khajehpour, S., Hearn, N., Pantazopoulou, S., & Sheikh, S., “Accelerated corrosion and repair of reinforced concrete columns using carbon fibre reinforced polymer sheets,” *Can. J. Civ. Eng.*, vol. 27, no. 5, pp. 941–948, Oct. 2000, doi: 10.1139/l00-030.
[10] K. W. Neale, M. Demers, and P. Labossiere, “FRP protection and rehabilitation of corrosion-damaged reinforced concrete columns,” *International Journal of Materials and Product Technology*, vol. 23, no. 3–4, pp. 348–371, Jan. 2005, doi: 10.1504/IJMPT.2005.007735.
[11] M. S. Radhi, M. S. Hassan, and I. N. Gorgis, “Carbon fibre-reinforced polymer confinement of corroded circular concrete columns,” *Journal of Building Engineering*, vol. 43, p. 102611, Nov. 2021, doi: 10.1016/j.jobe.2021.102611.
[12] S. P. Tastani and S. J. Pantazopoulou, “Experimental evaluation of FRP jackets in upgrading RC corroded columns with substandard detailing,” *Engineering Structures*, vol. 26, no. 6, pp. 817–829, May 2004, doi: 10.1016/j.engstruct.2004.02.003.
[13] S.-W. Bae and A. Belarbi, “Effects of Corrosion of Steel Reinforcement on RC Columns Wrapped with FRP Sheets,” *Journal of Performance of Constructed Facilities*, vol. 23, no. 1, pp. 20–31, Feb. 2009, doi: 10.1061/(ASCE)0887-3828(2009)23:1(20).
[14] P. Li, Y. Ren, Y. Zhou, Z. Zhu, and Y. Chen, “Experimental study on the mechanical properties of corroded RC columns repaired with large rupture strain FRP,” *Journal of Building Engineering*, vol. 54, p. 104413, Apr. 2022, doi: 10.1016/j.jobe.2022.104413.
[15] C. Hou, “Axial compressive behavior and model analysis of BFRP-jacketed corroded and pre-damaged circular reinforced concrete columns,” *Engineering Structures*, 2024.
[16] J. Zhu, M. Su, J. Huang, T. Ueda, and F. Xing, “The ICCP-SS technique for retrofitting reinforced concrete compressive members subjected to corrosion,” *Construction and Building Materials*, vol. 167, pp. 669–679, Apr. 2018, doi: 10.1016/j.conbuildmat.2018.01.096.
[17] J.-H. Zhu, Z. Wang, M. Su, T. Ueda, and F. Xing, “C-FRCM Jacket Confinement for RC Columns under Impressed Current Cathodic Protection,” *J. Compos. Constr.*, vol. 24, no. 2, p. 04020001, Apr. 2020, doi: 10.1061/(ASCE)CC.1943-5614.0001006.
[18] Y. Alhoubi, A. El Refai, F. Abed, T. El Maaddawy, and N. Tello, “Strengthening Pre-Damaged RC Square Columns with Fabric-Reinforced Cementitious Matrix (FRCM): Experimental Investigation,” *Composite Structures*, vol. 294, p. 115784, May 2022, doi: 10.1016/j.compstruct.2022.115784.
[19] N. Tello, F. Abed, A. ElRefai, T. El-Maaddawy, and Y. Alhoubi, “Experimental investigation of pre-damaged circular RC columns strengthened with fabric-reinforced cementitious matrix (FRCM),” *Structural Concrete*, vol. 24, no. 1, pp. 1656–1669, 2023, doi: 10.1002/suco.202200333.
[20] K. Toska, F. Faleschini, M. Zanini, L. Hofer, and C. Pellegrino, “Repair of severely damaged RC columns through FRCM composites,” *Construction and Building Materials*, vol. 273, Dec. 2020, doi: 10.1016/j.conbuildmat.2020.121739.
[21] Ö. Mercimek, A. Celik, R. Ghoroubi, and Ö. Anil, “Retrofitting of squat RC column by using TRM strip under axial load,” *Structures*, vol. 60, p. 105909, Jan. 2024, doi: 10.1016/j.istruc.2024.105909.
[22] J. Donnini, S. Spagnuolo, and V. Corinaldesi, “A comparison between the use of FRP, FRCM and HPM for concrete confinement,” *Composites Part B: Engineering*, vol. 160, pp. 586–594, Mar. 2019, doi: 10.1016/j.compositesb.2018.12.111.
[23] ASTM G01 Committee, *Practice for Preparing, Cleaning, and Evaluating Corrosion Test Specimens*. 2011.
[24] ACI committee 318, *ACI 318-19 Building Code Requirements for Structural Concrete*. 2019.
[25] Fabrics - SikaWrap® Hex-230 C – Sika Corporation - Sweets. Accessed: Oct. 30, 2024. [Online]. Available: https://sweets.construction.com/Manufacturer/Sika-Corporation-NST723/Products/Fabrics---SikaWrap-Hex-230-C-NST749787-P
[26] S&P ARMO-mesh® | S&P Clever Reinforcement. Accessed: Oct. 16, 2024. [Online]. Available: https://www.sp-reinforcement.eu/en-EU/products/sp-armo-meshr
[27] M. Elghazy, A. El Refai, U. Ebead, and A. Nanni, “Effect of corrosion damage on the flexural performance of RC beams strengthened with FRCM composites,” *Composite Structures*, vol. 180, pp. 994–1006, Nov. 2017, doi: 10.1016/j.compstruct.2017.08.069.
[28] S. R. Razvi and M. Saatcioglu, “Strength and Deformability of Confined High-Strength Concrete Columns,” *SJ*, vol. 91, no. 6, pp. 678–687, Nov. 1994, doi: 10.14359/1499.